**Paper 110**


Proceedings of the Eleventh International Conference
on Computational Structures Technology,
B.H.V. Topping, (Editor),
Civil-Comp Press, Stirlingshire, Scotland

# Local Fatigue Analysis using a Long Term Monitoring System at the Trezói Railway Bridge

**F. Marques, C. Moutinho and Á. Cunha**
**FEUP, Faculty of Engineering**
**University of Porto, Portugal**

## Abstract

Within the context of fatigue assessment of metallic railway bridges, the phenomena of local fatigue can be of major importance to the safety evaluation of this kind of structure. Therefore, this paper reports research work carried out to characterize the dynamic and fatigue behaviour of the Portuguese Trezói riveted railway bridge, presenting studies concerning the assessment of the local vibration characteristics directly associated with local fatigue problems, and also the calculation of the residual fatigue life of the bridge. This study was supported by a long term monitoring of key elements and details and it was conceived to measure critical stress patterns using strain gauges placed in strategic locations. This research was developed by the Laboratory of Vibrations and Monitoring (ViBest) of FEUP, in cooperation with the Portuguese railway administration, in the framework of the European FADLESS Project.

**Keywords:** railway bridges, dynamic monitoring system, strain gauges, fatigue assessment, local vibration fatigue.

## 1 Introduction

The maintenance and safety of existing bridges is a great concern of railway administrations since it can lead to an optimized use of the corresponding budgets. In particular, the safety of old riveted railway bridges, built and placed into service at the end of the $19^{th}$ and beginning of $20^{th}$ centuries, deserve a particular attention, since they were designed taking into account traffic conditions completely different from those observed in the present days, both in terms of vehicle gross weight and frequency. The current design procedures were not yet fully developed or even did not exist in those times and engineers were not aware of some important phenomena such as fatigue and, in particular, such as local vibration fatigue. Since the majority of collapses in railway steel bridges is related to fatigue and to assure high safety

levels in old riveted steel bridges, railway authorities have to invest heavily in their maintenance and retrofitting [2]. In this context, knowledge of the local dynamic behaviour and fatigue behaviour of riveted elements is of great importance.
The present paper reports research work carried out to characterize the dynamic and fatigue behaviour of the Portuguese Trezói riveted railway bridge, presenting studies concerning the assessment of the local vibration characteristics directly associated with local fatigue problems, and also the calculation of the residual fatigue life of the bridge. The study is supported by field measurements developed to characterize the strain patterns in the critical members.

## 2 Description of the bridge

The Trezói Bridge (Figure 1 a) is located in "Beira Alta" route, at the km 62 north of Mortágua in the village of Trezói. It was opened to traffic on the 20th August 1956. Its construction integrated the substitution of existing bridges in the "Beira Alta" route, carried out in the decade of 50. This substitution was funded by the Marshall Plan, and the German House Fried Krupp conceived, manufactured and mounted the 6 bridges of larger span of that Line, which led to the demolition of the previous ones, that where built by the Eiffel House [2].
It is a riveted metallic bridge with three spans of 39 m, 48 m and 39 m, totalizing 126 m length. The two inverted Warren truss girders that constitute the metallic deck of the bridge deck are 5.68 m height. The girders panels are 6.50 m wide in the central span and 6.00 m in the end spans. Two trapezoidal shape trusses acting as piers and two granite masonry abutments transmit the loads carried by the structure to the foundation. The deck has a constant width of 4.40m, throughout its length.
The superstructure bearing supports are metallic and allow free rotations in the structure plane. At the east support the longitudinal displacements are constrained while at the west they are permitted to embrace the deformations caused by longitudinal horizontal forces (thermal actions, braking, etc.).
The cross girders as well as the stringers resting on them were built using "I-shaped" sections. The cross girders have 71 cm height and are connected to the lateral vertical elements with riveted plates as shown in Figure 1 b). The chords and diagonals of the truss girders are formed by double "U-shape" sections. The two stringers that carry the live loads are aligned with the rails of the single track.

Figure 1: The Trezói Bridge: a) global view; b) View from inside the deck.

# 3 Numerical analysis

## 3.1 Global finite element models

In order to conduct the fatigue analysis, different numerical models have been developed using the software SOLVIA and ANSYS® 12.0 [1]. Bar and shell elements were used to develop the global model of the bridge and models of local details (Figures 2, 3 and 4).

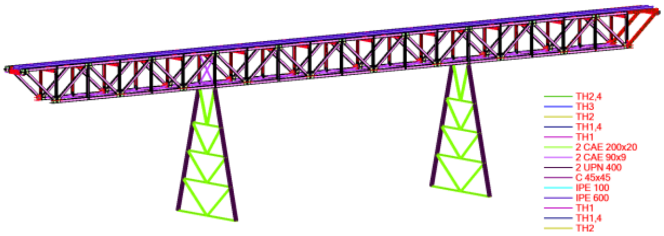


Figure 2: Global view of the shell finite element model.

In a first stage, a less time consuming numerical model was developed using only bar finite elements [2]. This model permitted the use of complex methodologies based on contact surfaces to simulate train crossing which are very demanding in terms of computer memory [1].

## 3.2 Local finite element models

The finite element model developed using beam elements was enhanced in order to capture local vibration modes. In that context, shell elements were used to simulate the structural elements that seemed to have higher stress ranges and higher damage values. A special attention was given to the joints of the cross girders, as seen in Figure 3, in order to capture local vibration modes, the effect of secondary bending moment and eventual distortion.

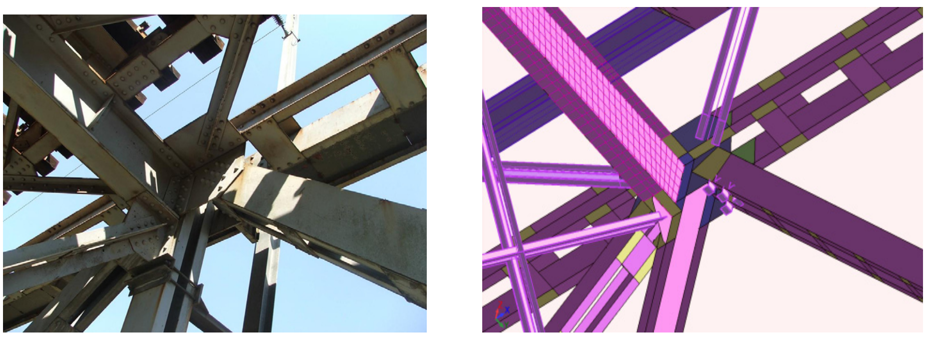

Figure 3: Finite element model using beam and shell elements

The model was refined at the vicinity of the cross girders above the piers, since it was clear that the cross girders played a major role in the local fatigue behaviour of this bridge. In Figure 4 we can observe the finite element model developed using bar elements for the majority of the elements and shell elements for the cross girders at the vicinity of the pier since it is at these structural elements that the highest damage is present.

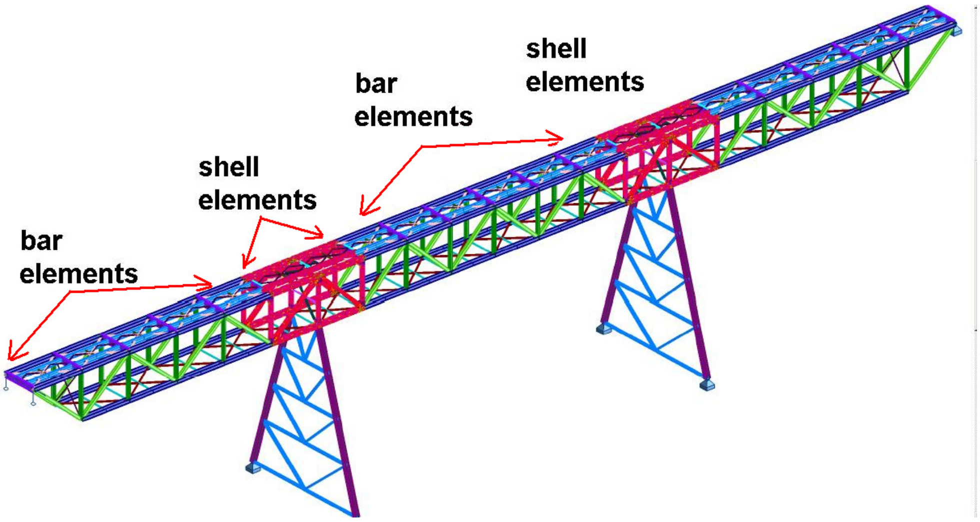


Figure 4: Finite element model using beam and shell elements for the cross girders

In Figure 5 we can see in more detail the structural model in the vicinity of the critical elements for local vibration fatigue and where shell elements were used. All secondary elements were modelled in order to characterize the real behaviour of this structural detail.

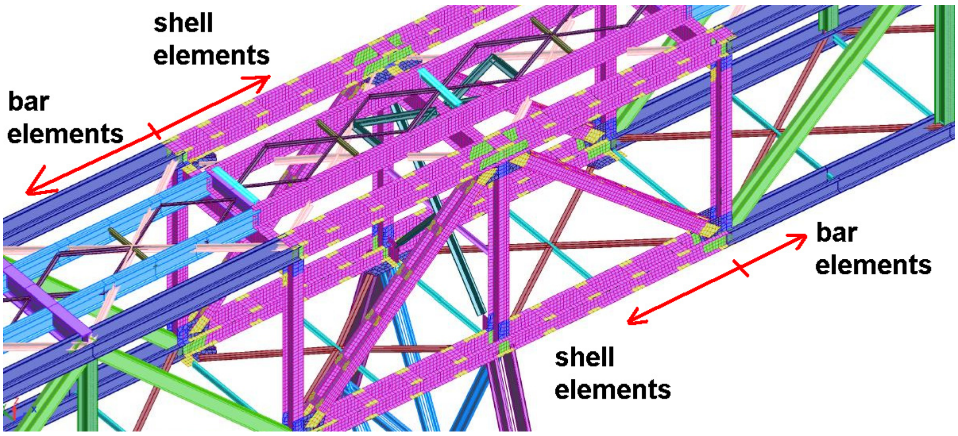


Figure 5: Finite element model using beam and shell elements, local view.

The longitudinal girders that support the rails were also modelled with shell elements, so that the connection between the flange of these elements and the flange of the cross girders was modelled in order to capture distortion effects. Rigid links were introduced between the nodes connecting the bar elements with the correspondent shell element that constitutes the top chord to simulate accurately the continuity between structural joints.

The same type of finite element model was developed to capture local vibration phenomena related to the cross-girders at the extremity support. These cross-girders are typically the structural elements with the highest damage since they experience higher number of stress cycles due to their sensitivity to the loads of each axle.

## 3.3 Local dynamic and fatigue analysis

To conclude about the local vibration modes that contribute the most for vibration induced fatigue, an analysis of the stress history calculated at the location of stress concentration was conducted. This stress concentration is present in the vicinity of the riveted connection between the top flange of the cross girder and the top chord as can be observed in Figure 6. This location corresponds to the spot where the stress is higher and the fatigue resistance is lower.

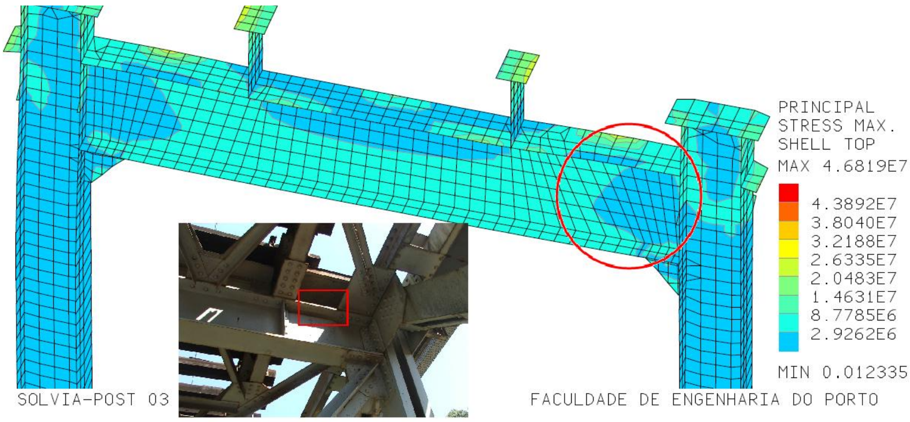


Figure 6: Location of maximum damage at the cross girder above the column.

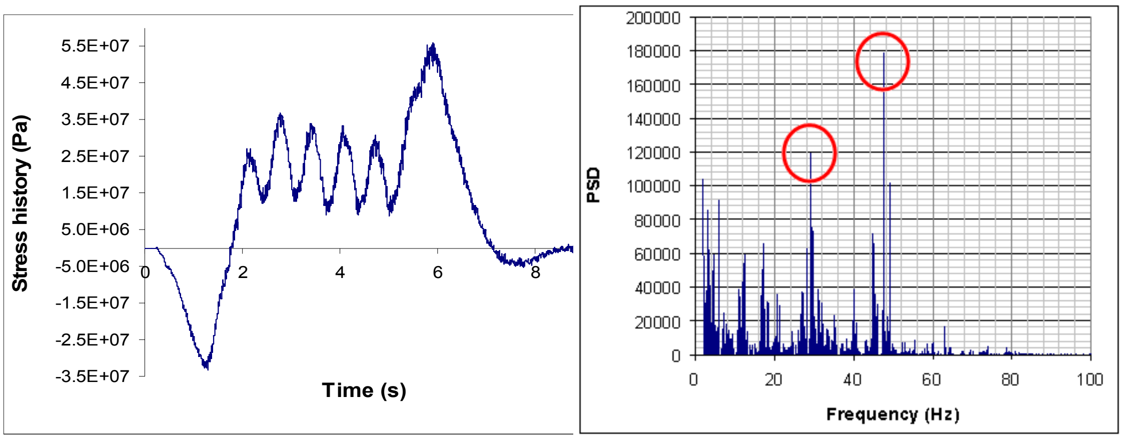


a) b)

Figure 7 – Frequency analysis of the stress-time history: a) Stress history at the cross girder above the column; b) Frequency content of the signal

In that context, a frequency domain analysis was performed for the stress history calculated (Figure 7 a)). This analysis allowed to conclude that there is a high influence of the local mode within the frequency ranges of 25-35 Hz and 45-55 Hz, as illustrated in Figure 7 b). We concluded that these frequencies correspond to some of the local modes of the cross girders presented in the next sections.

The same analysis was made for the vertical acceleration at the same location. In this case, the identification of the local modes which have the highest influence on the acceleration response is not so clear. However, it is still possible to identify some prominent peaks in the frequency content which correspond to a higher contribution of these frequencies to the structural response. These results are presented in Figure 8 where the same frequency ranges appear to be important.

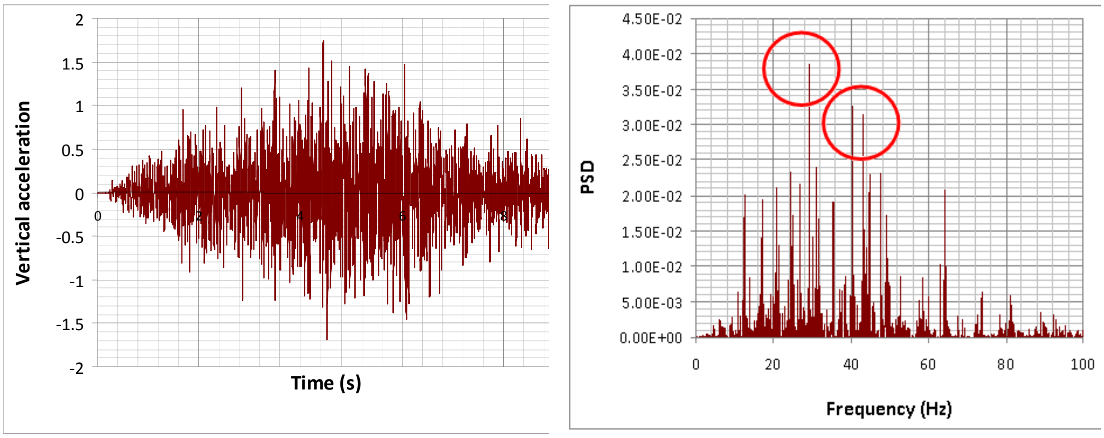


a) b)

Figure 8: Frequency analysis of the acceleration: a) acceleration at midspan of the cross girder above the column; b) Frequency content of the signal.

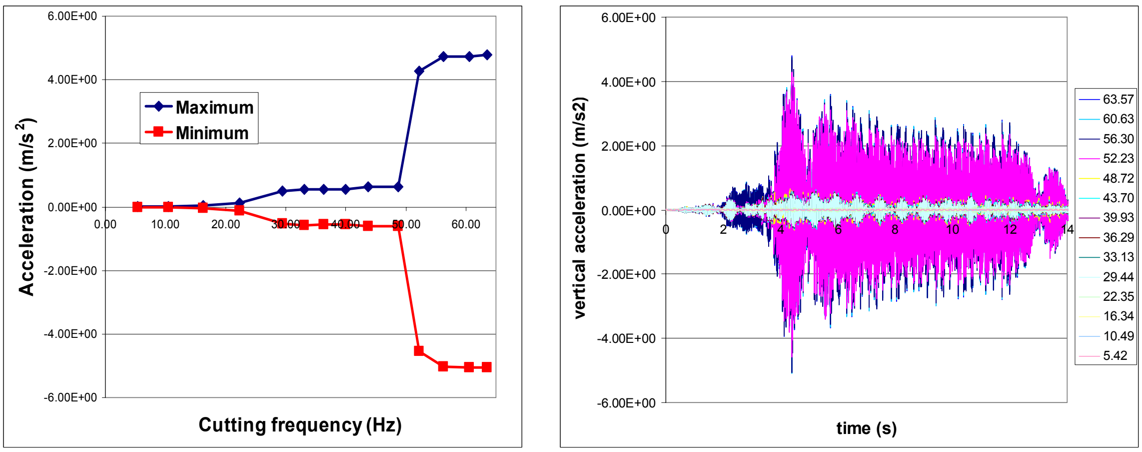


a) b)

Figure 9: Acceleration at midspan of the extreme cross girder: a) Maximum acceleration vs. Cutting frequency; b) Acceleration vs. time vs. cutting frequency

It was necessary to understand the influence of these modes on the dynamic response of the bridge. Several dynamic analyses were conducted with increasing number of modes included in the modal analysis. The lowest cutting frequency is 5 Hz, which doesn't include the first global bending mode of the bridge, and the highest frequency is 65 Hz, which includes all the main global modes and also the local modes of the cross-girders.

We can see in Figure 9 a) the effect of the cutting frequency in the extreme values of the vertical acceleration at midspan of the cross girder at the extreme support. Clearly there is a very high increase in the minimum and maximum values of the acceleration around the frequency of 50 Hz. This is easy to understand because the there are some important local bending modes of this element close to this value.

The influence of the local modes on the fatigue was evaluated by calculating the damage of the cross girders using a simpler model with beam finite elements and comparing these results with the damage calculated using the stress spectra obtained from the shell elements model. The damage was calculated using traditional S-N curves.

In Figure 10 b) we can see the stress spectrum obtained using shell elements and we can observe that there are a higher number of cycles for lower stress ranges. Figure 10 a) shows the damage calculated for the cross girders and for a freight train for different cutting frequencies and for bar and shell models. We can see that the damage has a small variation for almost all the frequencies for the case of the bar model. However, for the case of the shell model there is a very high increase of the damage which is precisely the modes corresponding to the cross girders. The same effect can bee seen in Figure 10 b), where the stress spectrum is presented.

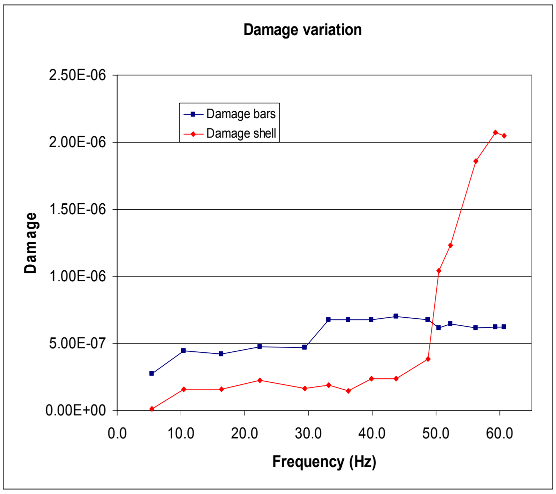


a)

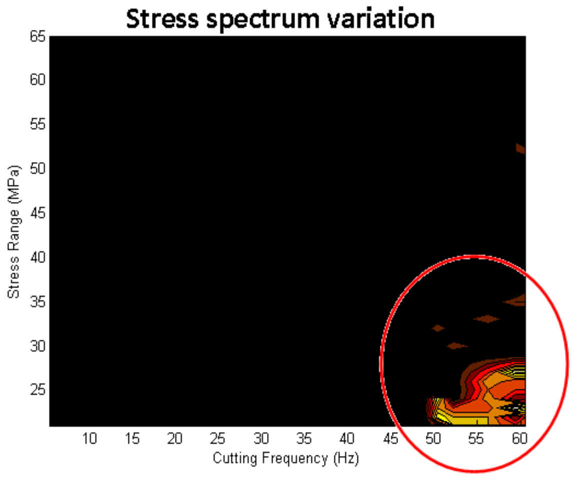


b)

Figure 10: Analysis of the influence of the cutting frequency on the damage evaluation: a) Damage *vs* cutting frequency; b) Stress spectra *vs* cutting frequency.

# 4 Field measurement campaigns

## 4.1 Ambient vibration test

An ambient vibration test was carried out with the objective of adjusting the numerical finite element model, modifying if necessary the model's mechanical characteristics, the distribution of mass or the support conditions.

The choice of seismographs (Figure 11) for the field measurements appeared to be the most adequate, since the units are completely independent between them and of any external source, they possess internal batteries, the collected information is kept in an internal memory unit and its synchronization is assured by GPS sensors, thus eliminating the necessity of electric cables.

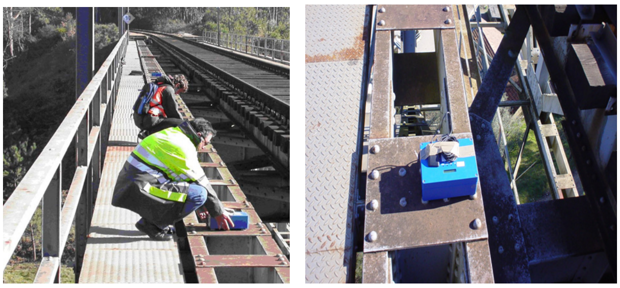

Figure 11: Placement of the seismographs.

Figures 12, 13 and 14 and Table 1 show some of the frequencies and modal configurations identified by the peak picking method. These results were compared with the values got from the numerical finite element model. The distinction between vertical and torsional modes was made using the simultaneous measurements at both sides of the bridge in the reference section, which led to the conclusion that the frequencies 6.01 Hz and 10.13 Hz are associated to torsional modes. Observing these results, it can be concluded that the correlation between identified and calculated natural frequencies is very good, presenting essentially some discrepancies in frequencies related with lateral modes. It's worth noting, however, that for the type of simulated actions (train vertical forces), the most important modes are the vertical ones.

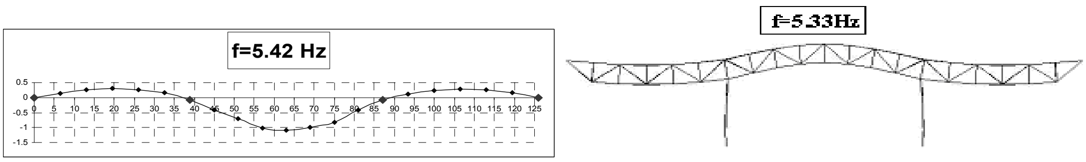


Figure 12: Identified *vs* calculated vertical modes.

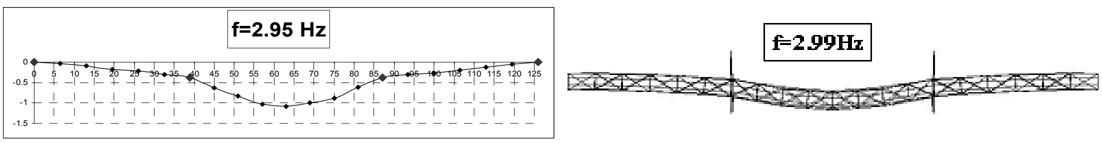


Figure 13: Identified *vs* calculated lateral mode.

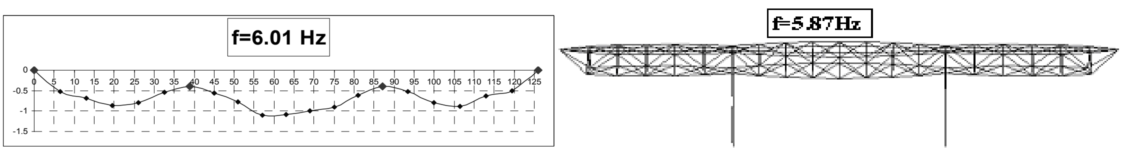


Figure 14: Identified *vs* calculated torsional mode.

| Identified frequency (Hz) | Calculated frequency (Hz) | Mode type | Variation % |
|---|---|---|---|
| 2.95 | 2.99 | $1^{st}$ transversal | 1.34 |
| 5.42 | 5.33 | $1^{st}$ vert. bending | 1.69 |
| 6.01 | 5.87 | $1^{st}$ torsional | 2.39 |
| 6.84 | 6.76 | $2^{nd}$ vert.bending | 1.18 |

Table 1: Calculated and identified frequencies.

The global vibration modes were compared and some slight modifications were made in order to achieve better agreement between the calculated and measured modal shapes and natural frequencies.

## 4.2 Temporary monitoring campaign

### 4.2.1 Description of the instrumentation

A field strain measurement campaign was also conducted at Trezói bridge using electrical strain gauges in order to characterize the local and global structural behaviour, and thus to enable the improvement and validation of the numerical models and simulations developed so far, to check stress paths and patterns in critical elements and connections, to obtain experimental stress histograms suitable for fatigue analysis and to gather data concerning the crossing vehicles in terms of speed, moving direction, number of axles and distances [3]. Sixteen sensors were applied to cross sections of bars which experience the higher tensile stress ranges and in rails sections in the vicinity of both abutments outside the bridge. Figure 15 illustrates the layout of the bridge instrumentation.

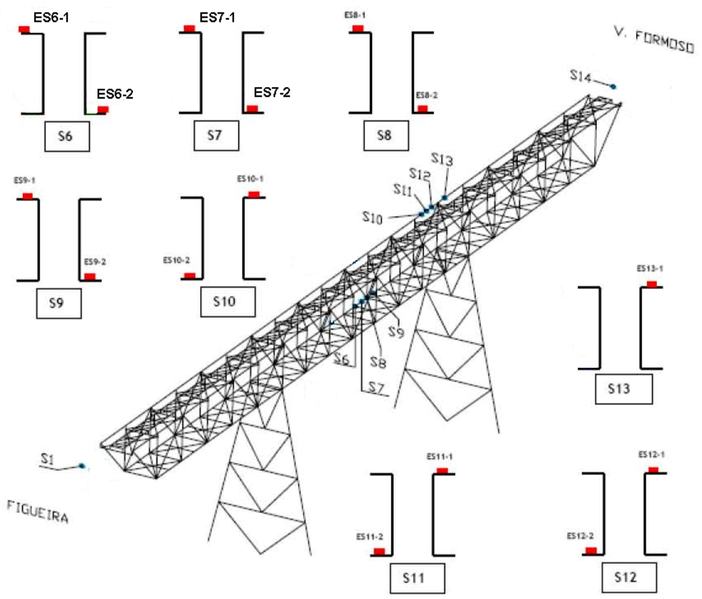


Figure 15: Instrumentation system: location of the 10 instrumented sections and corresponding distribution of the sensors

In some cases, the location of the sensors was defined to capture the local enhancement effect due to geometry stress concentration (Figures 16) and also, in general, to capture nominal stress.

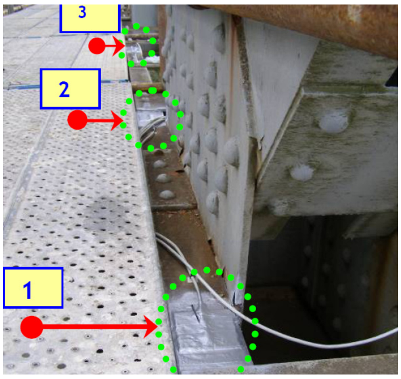


Figure 16: Lower joint of the truss girder instrumented with strain sensors.

### 4.2.2 Strain measurements and analysis

The measurements were performed in particular during two days that historically have higher traffic volume. During that period, 8 freight trains and 16 passenger trains crossed the bridge. As was stated previously, the contribution of REFER and CP (Portuguese railway agencies) made possible the simulation of the crossing by real trains, therefore the majority of geometrical characteristics and loads of the vehicles that crossed the bridge during the measurement period were known. In this context, a comparison between numerical and experimental stresses was made. Further analyses were made in order to calibrate and validate the numerical model using the field measurement campaign with strain gauges. The stresses measured at the top chord at the vicinity of one of the pier were compared with the corresponding stresses calculated. In Figure 17 the location of this strain gauge and the corresponding location of the calculated stresses in the finite element model are presented. The train that crossed the bridge at the time of the measurement was composed by a Locomotive and 4 passenger vehicles. The axle loads and spacing was already known due to the collaboration with the railway administration hence allowing the numerical simulation of the crossing.

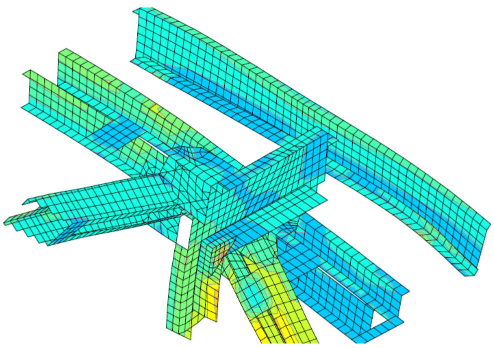

Figure 17: Location of strain gauges used to calibrate the numerical model and correspondent finite element model.

The results obtained are presented in Figure 18 a). The red graphic corresponds to the measured stresses and the blue to the calculated ones. Stresses in the direction of the longitudinal axle of the top chord were compared, which in this case correspond to the X axle. As we can observe in this Figure, the agreement between the two is very good. We also concluded that there was no need to further refine the mesh of the model in order to capture a good time history. Also in Figure 18 b) we can observe the damage calculated with the measured strains, and we could conclude that it is lower than the damage calculated using the Eurocode fatigue trains [1].

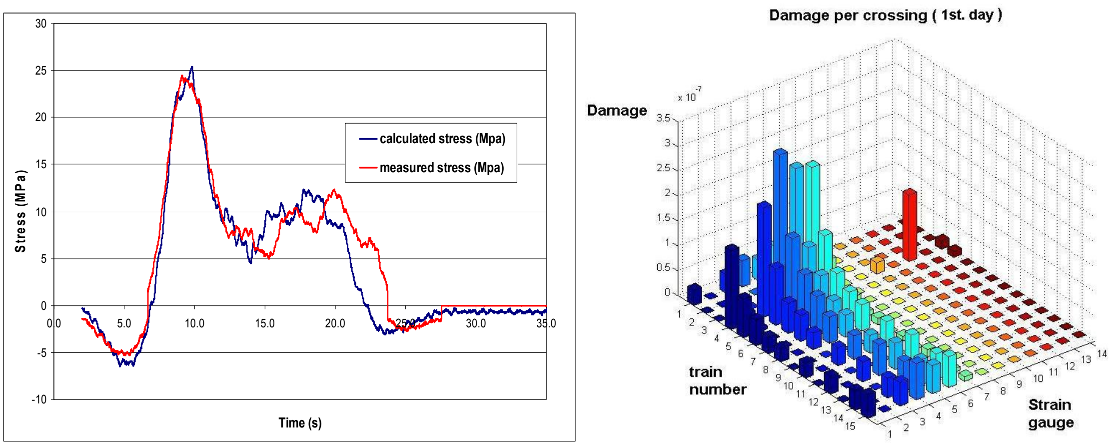


a) b)

Figure 18: Results of the measurement campaign: a) comparison between measured and calculated stresses; b) damage calculated with the strain measured.

## 4.3 Long term monitoring campaign

### 4.3.1 Previous work used as a basis for the development of the long term monitoring campaign

Figure 19 presents the results of the fatigue analysis developed on all structural elements of this bridge, which was conducted in previous studies [1].

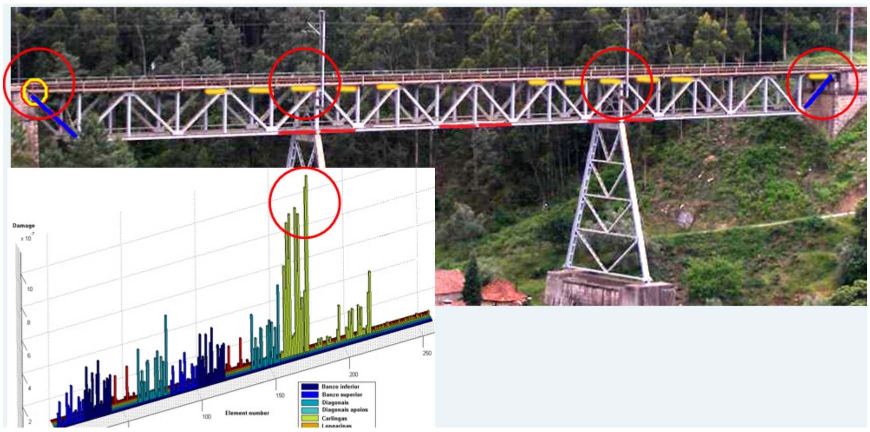

Figure 19 – Fatigue assessment results obtained using S-N curves and Miner rule

Observing this Figure, it is clear that the elements with the highest damage values (the yellow bars in the graphic) are the cross-girders above the central column and the cross-girders at the extremity supports. These results were the basis for the development of the experimental analysis of the local behavior.

### 4.3.2 Long term strain measurement system implementation

A long term monitoring system based on strain gauges was implemented. Strain gauges were applied in the cross girders located at the top of the piers and at one support in the abutment. In addition, rails sections in the vicinity of both abutments, but outside the bridge, were instrumented with strain gauges in order to estimate the axle loads of the real trains and the corresponding velocity. We can see the general layout of the instrumented sections in Figure 20.

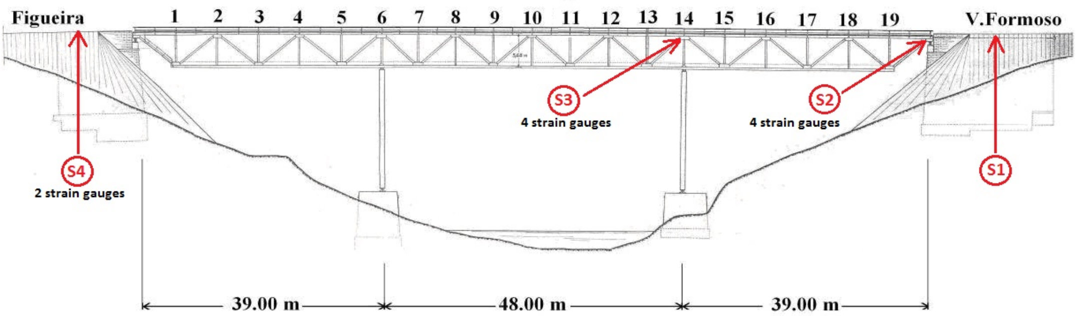


Figure 20: Global view of the location of strain gauges.

One of the most important aspects in the assessment of old structures is the estimation of real loadings. A more precise fatigue life can be calculated in the presence of more realistic stress spectra associated to these loadings. To this end and as stated above, the monitoring system was designed to allow the collection of data on vehicle characteristics, including the velocity spectra, number of axles, axle loads and their spacing, the moving directions and traffic density.
By observing Figure 21 it is possible to perceive that the strain gauges were placed at the bottom of the rails at the mid span between the wood sleepers in order the measure the maximum strains due to the train loads.

Figure 21: Location of strain gauges at the rails.

In Figure 22 a), we can observe the location of the strain gauges that were placed at the cross girder at the west extremity support. Four strain gauges were placed in the flanges of this element in order to capture the highest stress ranges at the detail with the lowest fatigue strength. The same layout was used for the cross girder above the central column (Figure 22 b)).

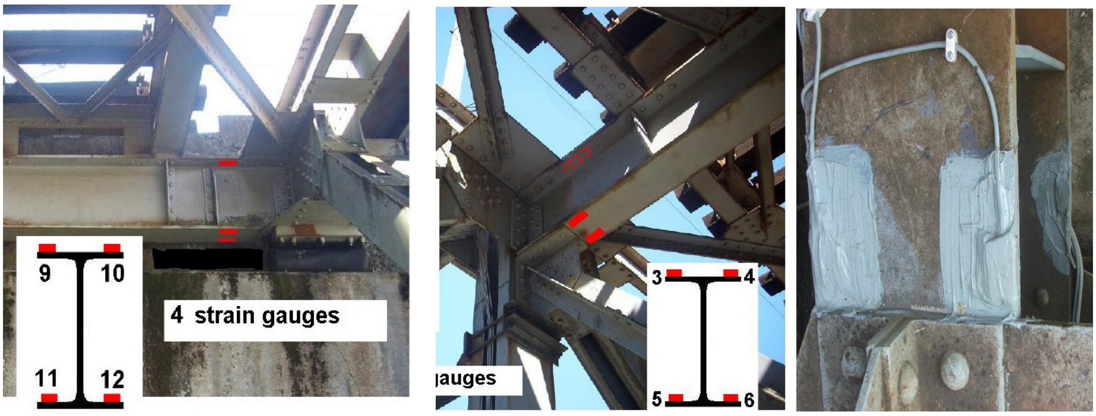


a) b) c)

Figure 22: Location of strain gauges at the cross-girders: a) extremity cross-girder; b) central cross-girder; c) partial view of the strain gauges

The acquisition system used was a platform from National Instruments and is composed by a computer responsible for high performance signal conditioning, which integrates two SCXI modules that are able to operate with 16 different channels. All this software is controlled by a Labview software which allows the storing, analysis and visualization of data and has also the advantage of being a graphical programming language enabling the development of user based routines. These features are presented in Figure 23. It this particular application only 12 channels were used and the data was acquired with a sampling frequency of 1000Hz.

Figure 23: Acquisition system: platform from National Instruments.

Due to the existence of noise detected in preliminary measurements (probably caused by electromagnetic interferences), an improvement of the connection to the

ground of the acquisition system was implemented in order to eliminate this problem. Five steel rods were wrapped with a copper wire and placed in a small pond filled with water. This wire was connected to the acquisition system.
This led to an immediate improvement of the signal measured by the strain gauges, reducing the noise amplitude by a factor of approximately 5. Also in the frequency domain, a clear improvement is observed.
Digital filtering was also used to increase the quality of the measured strains, particularly three digital notch filters were used to remove the influence of this noise in the structural response. This procedure was implemented in routines developed in Matlab environment and allows the elimination of a very narrow band of frequencies.

### 4.3.3 Measurement results and analysis

Some preliminary results have been obtained from a measurement period of 20 days. In Figure 24 we see an example of those results for the strain variations on the cross girders and on the rails. It is clear that the measured points have a logical pattern and describe adequately the rapid variation of the strains during the train crossing. The locomotive and wagons are in most cases identifiable.

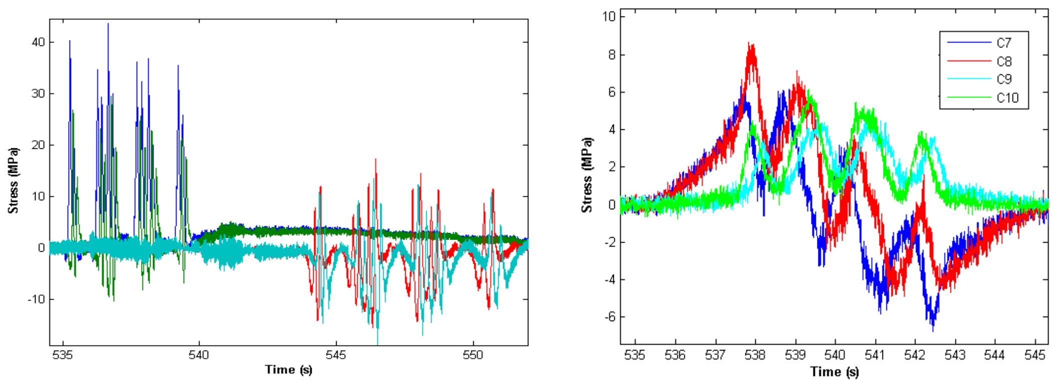


Figure 24: Stress time histories measured: a) at the rails; b) at the cross girder.

As referred previously, four strain gauges were placed at the rail sections at the vicinity of the abutments at the beginning of the bridge and at the end. These strain gauges were used to estimate the axle loads, axle spacing of the real trains and the correspondent velocity. A Weight in Motion algorithm was implemented in order to conduct these estimations. In this algorithm, the influence lines of the structural elements (in this case, the rails) are used to estimate the axle loads from strains. In order to identify the peaks that correspond to the wheel it was necessary to remove the values that correspond to noise and small vibrations that are not related directly with the axle load. To achieve that purpose, some routines in Matlab were developed. The signal was filtered with a Chebyshev Type II digital filter with a cutting frequency of 15Hz and an algorithm that removes local peaks with no physical meaning was implemented.

To estimate the velocity of the train, the distance between strain gauges was divided by the time that each axle takes to cross from one strain gauge to another. If the train is accelerating or braking it will be obtained a different velocity for each axle. In this work the mean velocity was analyzed. In Figure 25 we can observe the mean velocity and the axle spacing estimated for 415 trains.

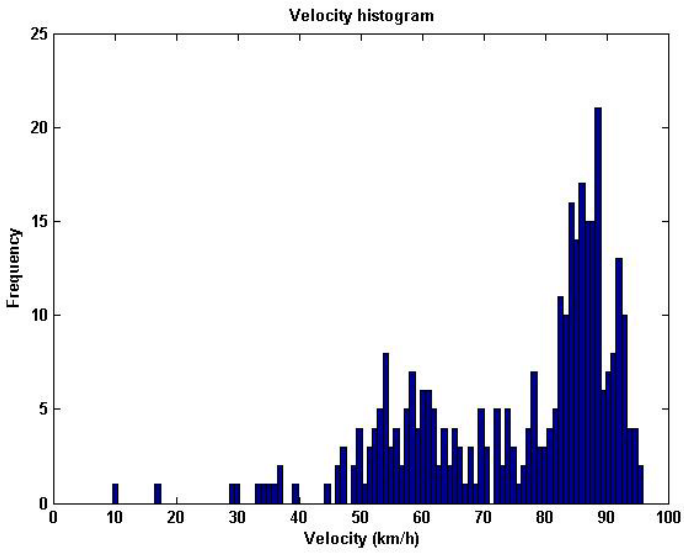


a)

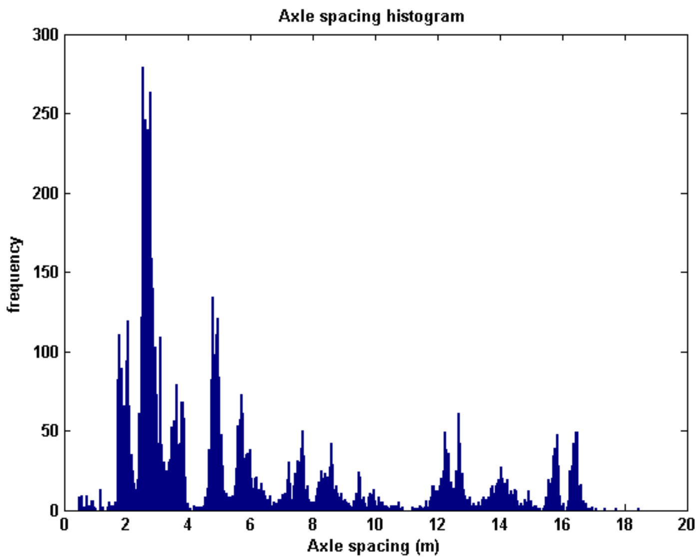


b)

Figure 25: Velocity and axle spacing estimation: a) mean velocity histogram; b) axle spacing histogram.

These results are logical since there is a maximum permitted velocity of 90km/h on the bridge, and there is a station very near the bridge which may lead to velocities within the range of 60km/h. The axle spacing histogram reveals the axle spacing of the bogies and the typical spacing of freight and passenger trains.

In order to estimate the axle loads, the methodology proposed in [4] was implemented. Assuming the structure to be linear, a set of loads $A_j$ located at a distance $x_i$ of the strain gauge will result in a strain ε in a structural element with an influence line I:

$$\varepsilon = \sum_i I(x_i) * A_j \tag{1}$$

The strain influence line was obtained by a 3D finite element model of the rail using volumetric elements, as can be observed in Figure 26.

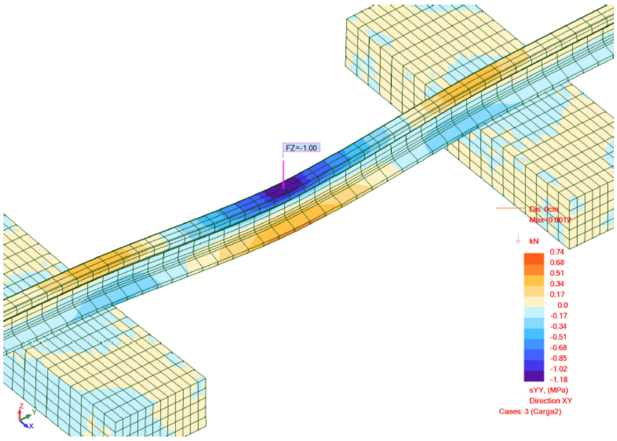

Figure 26: Finite element model of the rail.

In Figure 27 the axle loads estimated using this methodology is presented. The lower peak at the vicinity of 12 ton is related to passenger trains, since usually these vehicles have lower axle loads and high crossing frequency on this bridge. The peak at the vicinity of 16 ton is associated with freight trains.

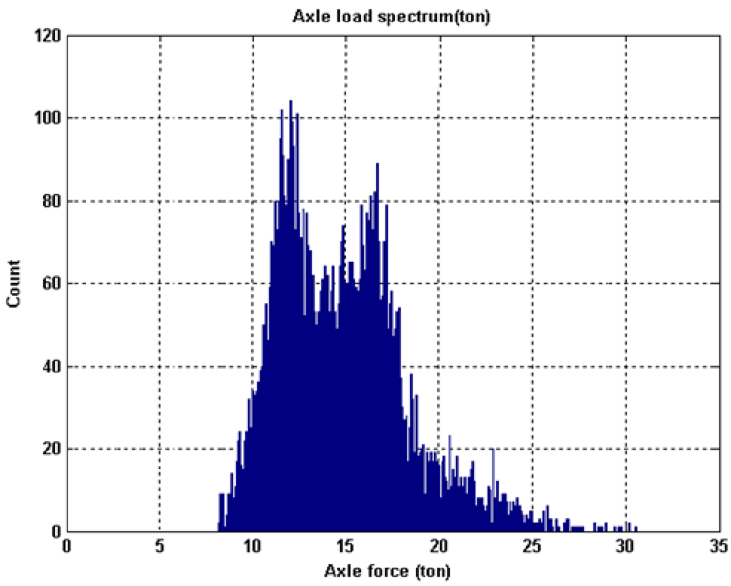


Figure 27: Histogram of the axle loads estimated

The Average Power Spectrum of the strain measured at the extremity cross girder, due to 415 trains that crossed the bridge during 20 days, was calculated in order to identify the frequencies that are present in the structural response. The resulting graphic is presented in Figure 28.

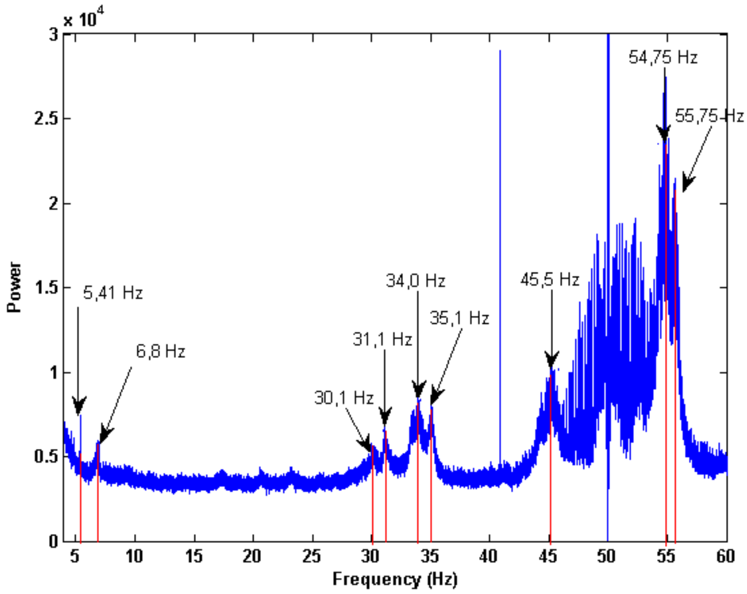


Figure 28: Average power spectrum of the strain measured at the extremity cross girder

Clearly, the first two global bending modes are identified in the lower frequency range in correspondence with the results obtained from the ambient vibration test performed. We can observe the first bending mode with a frequency of 5.42Hz and the second global bending mode with a frequency of 6.84Hz. The peaks with frequencies above 30Hz are associated with local vibration modes of the cross girders.

To evaluate the local dynamic behaviour of the elements of the bridge, a modal analysis of the numerical models described earlier was performed. These modal shapes were analysed in order to find the modes that have deformation patterns with stress enhancement that causes high local vibration fatigue. As was already exposed, the global vibration modes have frequencies within 2Hz and 10Hz. In opposition to these modes, we found that a very high number of local vibration modes of the deck are present in the range of frequencies between 10 Hz to 60 Hz, which revealed to be important to the dynamic response due to the train passage.

As concluded with Figure 28, it is interesting to observe that the structural behaviour of these secondary elements is influenced by global modes. However, it is easy to conclude that the local modes have a much higher influence. In many of those modes the main cause of dynamic stresses in the spot where the strain gauges were placed is due to the vibration of the longitudinal girders that support the rails. The secondary deformation caused by them in the cross-girder leads to the high concentration stresses. In Figure 29, two examples of these local modes are presented.

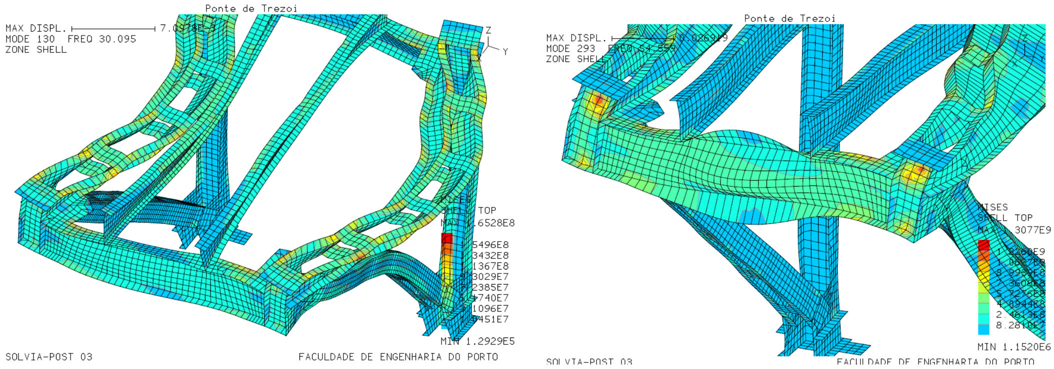


a) b)

Figure 29: Local vibration modes identified in the Average Power Spectrum: a) local bending mode of the cross girder with 30.1Hz; b) local bending and torsional mode with 54.56Hz.

Finally, the fatigue damage was calculated using these strain measurements for each of the 415 trains that crossed the bridge during a 20 days period. In this case, the S-N curves and the Miner rule were applied. In Figure 30 these results are presented, and we could conclude that the values are similar to the ones obtained using the numerical models, thus increasing the confidence in the analysis developed.

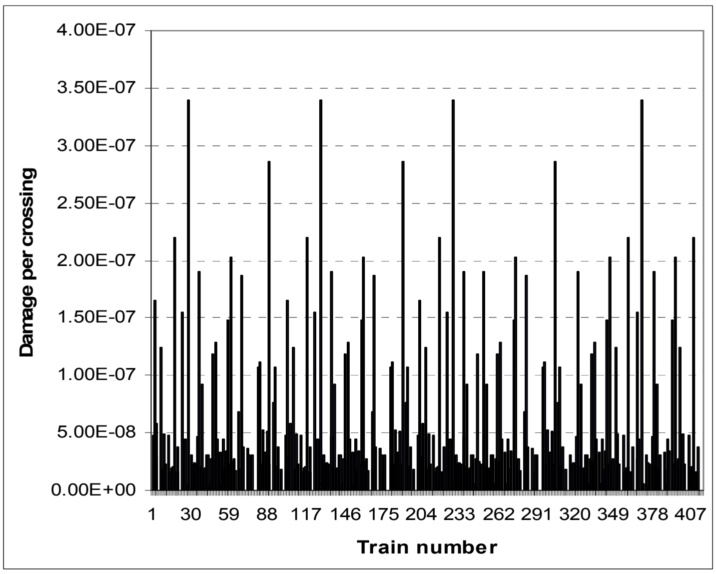


Figure 30: Fatigue damage for each of the measurements made.

# 5 Conclusions

This paper presents a study of the structural behaviour and fatigue assessment of the Trezói Bridge. Specifically, the local behaviour of critical details was analysed.
Several finite element models of the structure and details were developed using the SOLVIA software and two field measurement programmes were accomplished to update and validate the numerical model, as well as the numerical methodologies

used to simulate the trains crossings. The results obtained were used to understand local fatigue behaviour associated with the vibration phenomena.

## Ackowledgements

The authors acknowledge the financial support from RFCS (Research Fund for Coal and Steel) in the context of the European Project Fatigue Damage Controland Assessment for Railway Bridges (FADLESS), as well as from FCT.

## References

[1] Marques, F., Hu, W., Moutinho, C., Magalhães, F., Cunha, A. 2011. “Evaluation of dynamic effects and fatigue assessment of a railway bridge supported by temporary monitoring”. Eurodyn 2011 conference, Leuven.

[2] Marques, F. 2006. “Evaluation of dynamic effects and fatigue assessment in metallic railway bridges”. Master Thesis (in Portuguese), Faculty of Engineering University of Porto

[3] Labest. 2008. “Monitoring of the behaviour of Trezói railway bridge under dynamic loads”. Technical report (in Portuguese).

[4] Gonzalez, I. and Karoumi, R. 2011. “Traffic Monitoring Using a Structural Health Monitoring System”. Stockholm, Sweden.